



Montréal, Québec
May 29 to June 1, 2013 / 29 mai au 1 juin 2013

Comparison of wind tunnel results with Canadian provisions for wind-induced torsion on low- and medium-rise buildings

Mohamed Elsharawy, Khaled Galal and Ted Stathopoulos
Faculty of Engineering and Computer Science, Concordia University, Montréal, Québec, Canada H3G 1M8

Abstract: The aim of this study is to assess wind-induced torsional loads on low- and medium-rise buildings in the National Building Code of Canada (NBCC 2010). Two building models with the same horizontal dimensions but different gabled-roof angles (0° and 45°) were tested at different full-scale equivalent eave heights (6, 12, 20, 30, 40, 50, and 60 m) in open terrain exposure for several wind directions (every 15°). Wind-induced measured pressures were numerically integrated over all building surfaces and results were obtained for along-wind force, across-wind force, and torsional moment. Torsion load case (i.e. maximum torsion and corresponding shear) and shear load case (i.e. maximum shear and corresponding torsion) were evaluated to reflect the maximum actual wind load effects in the two horizontal directions (i.e. transverse and longitudinal). The evaluated torsion and shear load cases were also compared with the current torsion- and shear-related provisions in the NBCC 2010. The results demonstrated significant discrepancies between NBCC 2010 and the wind tunnel measurements regarding evaluating torsional wind loads on low- and medium-rise buildings. The paper provides suggestions to enhance the NBCC provisions for the evaluation of torsional loads on low- and medium-rise buildings.

1 Introduction

Proper building design against wind loads depends primarily on the adequacy of the provisions of codes of practice and wind load standards. During the past decades, much has been learned about along- and across-wind forces on buildings. However, studies on wind-induced torsional loads on buildings are very limited. The recent trend towards more complex building shapes and structural systems results in more unbalanced wind loads and larger torsional moments. Thus, re-visiting the wind load provisions is of an utmost concern to ensure their adequacy in evaluating torsion on low- and medium-rise buildings and consequently achieve safe yet economic building design. Particularly, most of the wind loading provisions on torsion have been developed from the research work largely directed towards very tall and flexible buildings (Melbourne, 1975, Vickery and Basu, 1984, and Boggs et al. 2000) for which resonant responses are very significant. However, the dynamic response of most medium-rise buildings is dominated by quasi-steady gust loading with little resonant effect. Moreover, the lack of knowledge regarding wind-induced torsion is apparent in the different approaches in evaluating torsion in the international wind loading codes and standards. Tamura et al. (2008) and Keast et al. (2012) studied wind load combinations including torsion for medium-rise buildings. The latter study concluded that for rectangular buildings the peak overall torsion occurs simultaneously with 30-40% of the peak overall shear, but tested only a limited number of building models. Additional experimental results for testing different building configurations are still required to confirm and generalize these results.

Furthermore, studies on wind-induced torsional loads on low-rise buildings are very limited. Isyumov and Case (2000) measured wind-induced torsion for three low-rise buildings with different aspect ratios

(length/width = 1, 2, and 3) in open terrain exposure as modeled in the wind tunnel. It was suggested that applying partial wind loads, similar to those implemented for the design of medium-rise buildings, would improve the design of low-rise buildings until more pertinent data become available. Tamura et al. (2001) examined correlation of torsion with along-wind and across-wind forces for rectangular low-rise buildings tested in simulated open and urban terrain exposures. Low-rise buildings of different roof slopes were also tested by Elsharawy et al. (2012). It was concluded that the peak torsions evaluated by current wind provisions are different from the measured peak torsion in the wind tunnel.

This paper reports the analysis and code comparison of results of additional measurements carried out in a boundary layer tunnel to investigate shear forces occurring simultaneously with maximum torsion, as well as maximum shears and corresponding torsions on buildings of different roof slopes and heights. Results of the study are important for the appropriate evaluation of wind-induced torsional loads on buildings.

2 Wind loads including torsion in NBCC 2010

The National Building Code of Canada was the first adopted in its provisions the effect of wind-induced torsional loads on buildings. Since the early 70's and till 2005, the NBCC subcommittee on wind loads introduced the unbalanced wind loads or wind-induced torsion on medium-rise buildings by removing 25% of the full wind load from any portion on building surfaces in order to maximize torsion according to the most critical design scenario states. This allowance for torsion is equivalent to applying the full design wind load at 3 or 4 percent of the building width. In the absence of detailed research in this area and based on some wind tunnel observations the 25% removal of the full wind load has been modified in the NBCC 2005 edition to a complete removal of the full wind loads from those areas that would lead to maximizing torsion. This allowance for torsion is equivalent to applying the full design wind load at 12.5 percent of the building width in case of loading half of the width of the building.

In the NBCC (2010), the static method specifies wind loads on low-rise buildings (defined as having mean roof height, $h < 10$ m, or $h < 20$ m and $h <$ smallest horizontal building dimension, B). One load case is described in the static approach to evaluate maximum shear as well as maximum torsion. The simplified method is suggested for medium-rise buildings, defined as having $h < 60$ m, $h/B < 4$, and lowest natural frequency, $f_n > 1$ Hz. The simplified method identifies four load cases. In Cases A and C, symmetric uniform loads are considered, in order to estimate the maximum base shears and overturning moments. On the other hand, partial wind loads are recommended to create equivalent torsional building loads in Cases B and D. Nevertheless, the choice of partial loads could be difficult for design engineers as can be seen from the code statements quoted below:

"In case B, the full wind pressure should be applied only to parts of the wall faces so that the wind-induced torsion is maximized" (note (2) to figure I-16); and

"... the influence of removing 50% of the case C loads from parts of the face areas that maximizes torsion, as shown in figure I-16, case D, should be investigated" (Commentary I, 37).

3 Wind tunnel tests

The experiments were carried out in the boundary layer wind tunnel of Concordia University. The working section of the tunnel is approximately 12.2 m long x 1.80 m wide. Its height is adjustable and ranging between 1.4 and 1.8 m to maintain negligible pressure gradient along the test section. A turntable of 1.2 m diameter is located on the test section of the tunnel and allows testing of models for any wind direction. An automated Traversing Gear system provides the capability of probe placement to measure wind characteristics at any spatial location around a building model inside the test section. A geometric scale of 1:400 has been recommended for the simulation of the most important variables of the atmospheric boundary layer under strong wind conditions.

3.1 Building Models

Figure 1 shows the two building models, with 0° and 45° gabled roof angels, and the location of 146 and 192 pressure taps on their surfaces respectively. The flat roof does not have any pressure taps, since

uplift forces do not contribute to torsion or horizontal shear forces. The models were tested at different building heights, by sliding it downwards in a precise tightly fit slot in the turntable, such that it represents four actual buildings with eave heights 6, 12, 20, 30, 40, 50 and 60 m. Model dimensions and the tested building heights are given in Table 1. In this study, all tested buildings were assumed to be structurally rigid and follow the limitations stated in the three wind load standards.

3.2 Terrain simulations

An open-country exposure was simulated in the wind tunnel. The flow approach profiles of mean wind velocity and turbulence intensity measured using a 4-hole Cobra probe (TFI) for the simulated terrain exposure (see Figure 2). The wind velocity at free stream was 13.6 m/s. The power law index α of the mean wind velocity profile was set at $\alpha = 0.15$. Although it is not common for medium height buildings to be situated in open terrain, this exposure was chosen as a kind of conservatism since higher loads are expected to act on the tested buildings in this case. The pressure measurements on the models were conducted using a system of miniature pressure scanners from Scanivalve (ZOC33/64Px) and the digital service module DSM 3400. All measurements were synchronized with a sampling rate of 300Hz on each channel for a period of 27 sec (i.e. about one hour in full scale). It is well known that the mean wind speed has the tendency to remain relatively steady over smaller periods of time (i.e. 10 minutes to an hour) assuming stationarity of wind speed, as reported by van der Hoven (1957). It is also worthy to mention that this period is considered suitable to capture all gust loads, associated with the fundamental building frequencies, which may be critical for structural design.

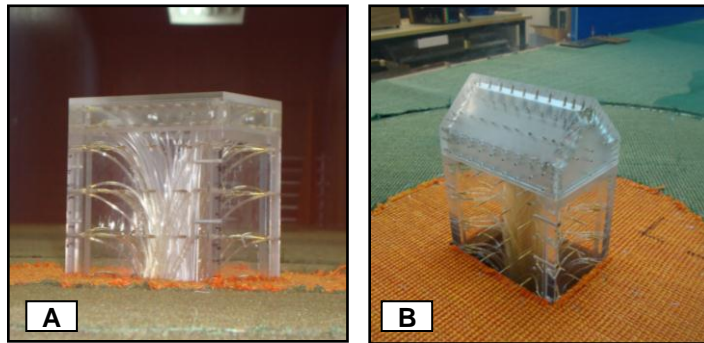


Figure 1: Wind tunnel buildings models:
A) Flat roof; B) Roof gable (45°)

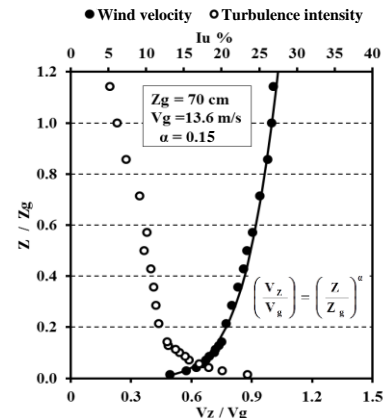


Figure 2: Wind velocity and turbulence intensity profiles for open terrain exposure

Table 1. Model dimensions and building heights tested in the boundary layer wind tunnel

Building	Dimensions	
	Scaled (1:400, mm)	Actual (m)
Width (B)	97.5	39
Length (L)	152.5	61
Tested heights (H)	15, 30, 50, 75, 100, 125, and 150	6, 12, 20, 30, 40, 50, and 60

4 Analytical methodology

Figure 3 shows a schematic representation of external pressure distributions on building envelope at a certain instant, the exerted shear forces, F_x and F_y , along the two orthogonal axes of the buildings, as well as torsional moment, M_T , at the geometric centre of the building. Pressure measurements are scanned simultaneously. The instantaneous wind force at each pressure tap is calculated according to:

$$f_{i,t} = (p_{i,t} \times A_{\text{effective}}) \quad f_{j,t} = (p_{j,t} \times A_{\text{effective}}) \quad (1)$$

where $P_{i,t}$, and $P_{j,t}$ are instantaneous pressures measured at each pressure tap. The wind forces exerted at pressure tap locations in X- and Y-directions are noted by $f_{i,t}$ and $f_{j,t}$, respectively. For each wind

direction, the horizontal force components in X- and Y-directions and the total base shear are evaluated according to:

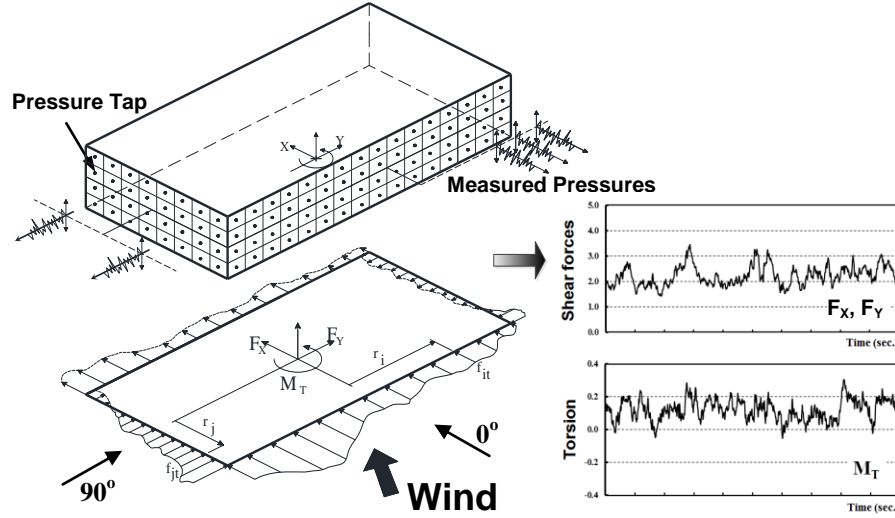


Figure 3: Measurement procedure for horizontal wind forces, F_X and F_Y , and torsional moment, M_T

$$F_X = \sum_{i=1}^N f_{i,t} \quad F_Y = \sum_{j=1}^M f_{j,t} \quad V = \sqrt{F_X^2 + F_Y^2} \quad (2)$$

where N and M are the numbers of pressure taps on the longitudinal and transverse directions, respectively. All these forces are normalized with respect to the dynamic wind pressure at the roof height as follows:

$$C_{sx} = \frac{F_X}{q_h B^2} \quad C_{sy} = \frac{F_Y}{q_h B^2} \quad C_V = \frac{V}{q_h B^2} \quad (3)$$

Where q_h = dynamic wind pressure (kN/m^2) at mean roof height h (m), B = smaller horizontal building dimension (m). The torsional coefficients, C_T , and equivalent eccentricity, e , are evaluated based on:

$$C_T = \frac{M_T}{q_h B^2 L} \quad e_x (\%) = \frac{M_T}{L * V} * 100 \quad e_y (\%) = \frac{M_T}{B * V} * 100 \quad (4)$$

where L = longer horizontal building dimension

The measured peak shear forces and torsional moment presented herein are calculated as the average of ten critical values (keast et al. (2012)). Also the corresponding shear and torsion were evaluated as the average of ten values corresponding to the ten peaks. This is associated with a probability of exceedence less than 0.1%.

5 Experimental results

Figures 4 to 6 present the peak coefficients of torsion, shear in x-direction, and shear in y-direction measured when the two buildings were tested at different eave heights (H) for different wind directions. As expected, shear coefficient in x-axis decreases when incident wind angle varied from 0° to 90° , as shown in Figure 5. On the other hand, for the same wind range shear coefficient in y-axis increases. The maximum shear force in the x-direction occurs for wind direction ranging from 0° to 30° ; whereas in the y-direction for wind almost perpendicular to building face, (90°). It could be seen the significant effect of increasing the building heights and the roof slope on the generated torsion and shear forces. Changing

building eave height from 6 to 60 m resulted in increasing torsion and shear coefficients about 12 and 5 times for buildings with 0° and 45° roof angles respectively. Changing the roof angle from 0° to 45° for buildings tested at different eave height results in an increase of the torsion and shear coefficients by about 50%.

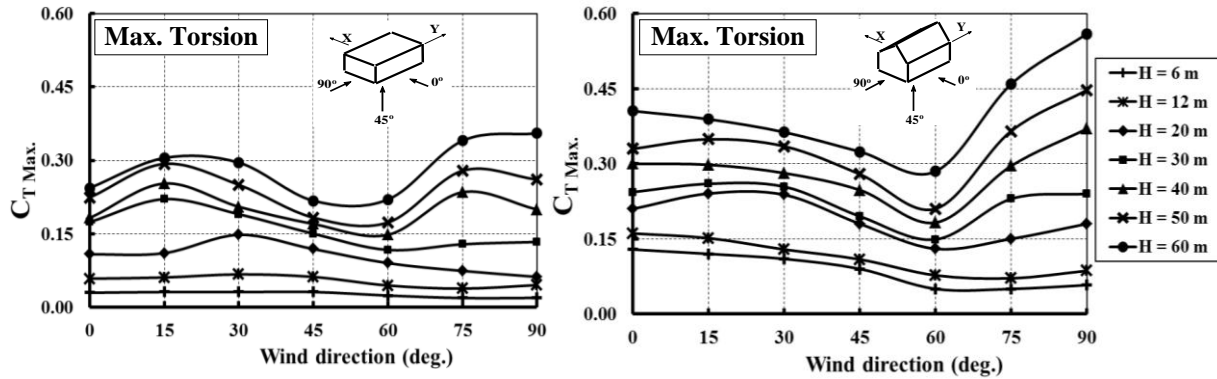


Figure (4): Variation of peak torsion coefficient ($C_{T \text{ Max.}}$) with wind direction for the tested buildings

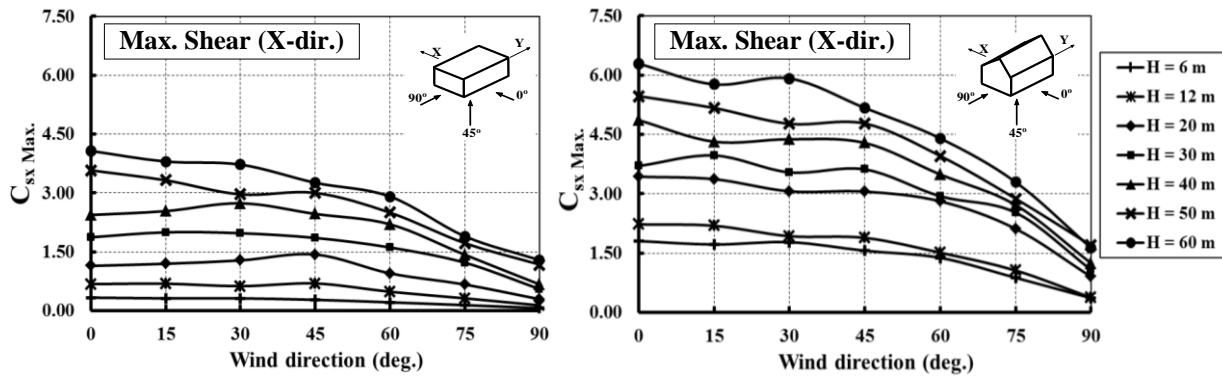


Figure (5): Variation of peak shear coefficient ($C_{Sx \text{ Max.}}$) with wind direction for the tested buildings

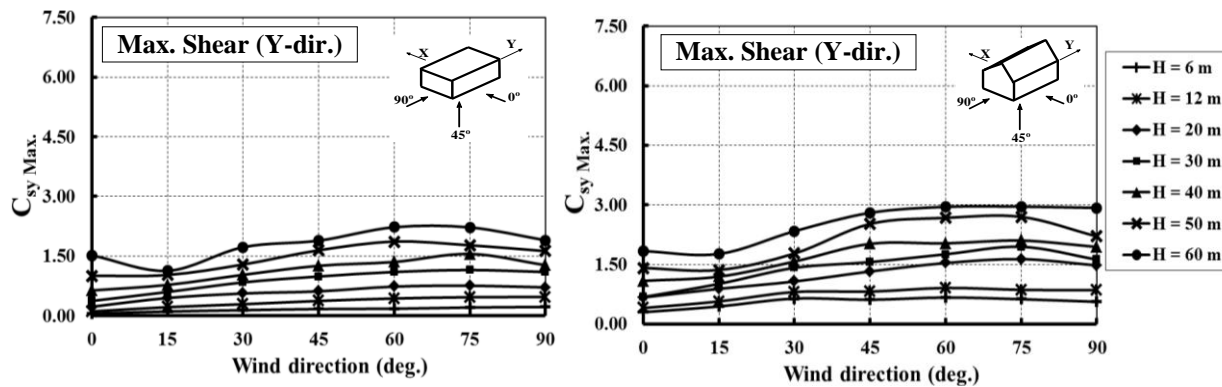


Figure (6): Variation of peak shear coefficient ($C_{Sy \text{ Max.}}$) with wind direction for the tested buildings

6 COMPARISON WITH PREVIOUS STUDIES

A comparison of the results with those from a previous study by Keast et al. (2012) for a building with a flat roof and dimensions $L = 40 \times B = 20 \times H = 60$ m was made using the wind tunnel measurements in the current study for a building model with $L = 61 \times B = 39 \times H = 60$ m. The Keast et al. (2012) study

has used shear and torsional coefficients defined as; $C_v = \text{Base shear}/(q_H LH)$ and $C_T = \text{Base torsion}/(q_H L^2H)$, respectively (where $q_H = \text{dynamic wind pressure at mean roof height}$, $L = \text{longer horizontal building dimension}$, $H = \text{eave building height}$). For comparison purposes, the results of the current study have been transformed to the same definitions of shear and torsional coefficients as used by Keast et al. (2012). Table 2 presents the experimental parameters as well as the evaluated shear and torsional coefficients for the studied buildings. Figure 7 shows the mean and maximum torsional coefficients for different wind direction evaluated by the three studies. Results show relatively good agreement for the measured shear forces and torsion in the three studies. The small differences could be attributed to the difference in building dimensions, the scale used, and the terrain exposure.

Table 2: Comparison with Keast et al. study (2012):

	Keast et al. 2012	Current study
Wind tunnel technique	A 6 degree-of-freedom high frequency balance	High frequency pressure integration
Building dimensions (m)	L = 40 x B = 20 x H = 60	L = 61 x B = 39 x H = 60
Aspect ratio (L/B)	2	1.60
Scale	1:400	1:400
Model dimensions (mm)	100 x 50 x 150	152.5 x 97.5 x 150
Terrain exposures	Open	Open ($\alpha=0.15$)
Wind direction	0° to 90° by 15°	0° to 90° by 15°
Torsional coeff. ($C_{T \max}$)	0.14	0.15
Shear coefficient ($C_{vx \max}$)	2.00	1.80
Shear coefficient ($C_{vy \max}$)	0.95	0.90

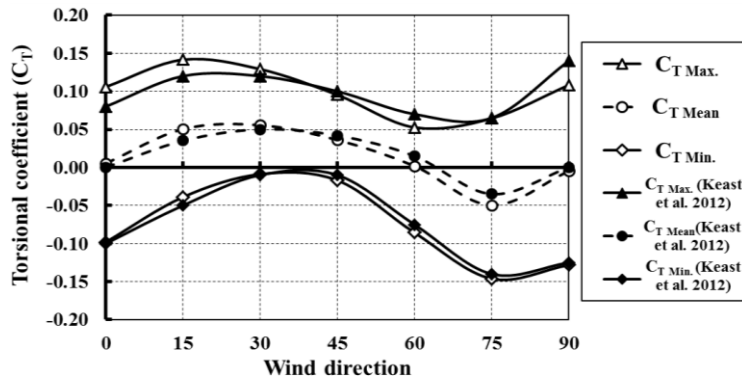


Figure 7: Torsional coefficient comparison for rectangular building with height 60 m located in open country

Another comparison with a previous study by Tamura et al., (2003) for a building with dimensions $L = 42.5 \times B = 30 \times H = 50$ m was made using a building model having $L = 61 \text{ m} \times B = 39 \text{ m} \times H = 50$ m. The two flat roof buildings have an aspect ratio of their plan dimension, $L/B \approx 1.5$. In this comparison, the definitions of torsional and shear coefficients in the Tamura et al. (2003) study were followed. The torsional coefficient was considered as $C_T = \text{Base torsion}/(q_H LHR)$ where; $R = \sqrt{(L^2 + B^2)}/2$, $B = \text{smaller horizontal building dimension}$, and shear coefficient $C_v = \text{Base shear}/(q_H LH)$. Tamura et al. 2003 study shows higher coefficients by about 60% (see Table 3), but this is likely due to the two different terrain exposures used in the two studies. Indeed, the mean wind velocity at the eave building height in urban terrain is much lower than in open terrain exposure.

7 COMPARISON WITH THE NBCC (2010)

The experimental results were used to introduce four load cases, namely: shear and torsion load cases in both transverse and longitudinal wind directions (see Table 4). These load case values were compared to the evaluated shear and torsion values by the NBCC (2010). In the shear load case, maximum shear was considered along with the corresponding torsion, whereas in the torsion load case, maximum torsion and the corresponding shear were evaluated.

Table 3. Comparison with previous study by Tamura et al. 2003

Experimental variables	Tamura et al. 2003	Current study
Wind tunnel technique	High frequency pressure integration	High frequency pressure integration
Building dimensions (m)	L = 50 x B = 25 x h = 50	L = 61 x B = 39 x h = 50
Aspect ratio (L/B)	2.0	1.6
Scale	1:250	1:400
Model dimensions (mm)	100 x 100 x 200	152.5 x 97.5 x 30
Terrain exposures	Urban ($\alpha = 0.25$)	Open ($\alpha = 0.15$)
Wind direction	\perp to building length (L= 50 m)	\perp to building length (L= 61 m)
Torsional coefficient ($C_{T \max}$)	0.30	0.20
Shear coefficient ($C_{vx \max}$)	3.00	1.90
Shear coefficient ($C_{vy \max}$)	0.90	0.50

In NBCC (2010), the static method, as mentioned earlier, is introduced for low-rise buildings while the simplified method is proposed for medium-rise buildings. The static method calculations for the torsional and shear coefficients were derived based on figure I-7 in Commentary I of NBCC 2010, where the external peak (gust) pressure coefficients ($C_p C_g$) are provided for low buildings. Likewise, for the simplified method, the external pressure is taken from figure I-15, Commentary I. Partial and full load cases were considered to estimate maximum torsion and corresponding shear, as well as maximum shear and corresponding torsion. Calculations were carried out considering the open terrain exposure. Static method values were increased by 25% to eliminate the implicit reduction (0.8) due to directionality.

Table 4. Wind load cases in transverse and longitudinal directions

	Transverse direction	Longitudinal direction
Shear load cases	Max. shear in X-dir. ($C_{sx \max}$), and corresponding torsion ($C_{T \text{ Corr}}$)	Max. shear in Y-dir. ($C_{sy \max}$), and corresponding torsion ($C_{T \text{ Corr}}$)
Torsional load cases	Max. torsion ($C_{T \max}$), and corresponding shear in X-dir. ($C_{Sx \text{ Corr}}$)	Max. torsion ($C_{T \max}$), and corresponding shear in Y-dir. ($C_{Sy \text{ Corr}}$)

Figure 8 shows the wind tunnel results along with the evaluated torsional load case parameters by the static and simplified methods in the transverse direction. Although the static method requires applying higher loads ($C_{v \text{ Corr}}$) in comparison with wind tunnel measurements, it significantly underestimates torsion ($C_{T \max}$) on low-rise buildings. This is mainly due to the fact that it specifies a significantly lower equivalent eccentricity ($e\%$) which is about 3% of the facing building's width compared to the equivalent eccentricity evaluated in the wind tunnel tests which is around 15%. On the other hand, for the building with flat roof, the simplified method requires applying almost the same wind loads as those measured in the wind tunnel. The eccentricity specified by the simplified method is 25% of the facing building width, which is significantly higher than the measured eccentricity (about 15%), hence the evaluated torsion using the simplified method exceeds the measured torsion significantly. For the building with 45° roof, the corresponding shear seems to exceed the corresponding shear on the flat roof building by 50%. However lower eccentricities were noticed for buildings with roof angle 45°. Figure 9 presents shear load case in the transverse direction evaluated by the NBCC (2010) and wind tunnel. The static method compares well with the wind tunnel measurements in evaluating maximum shear while underestimates the corresponding torsion on low-rise building with 45°. The simplified method overestimates shear on buildings with flat roofs, however it underestimates shear on building with 45° roof angle with heights up to 40m. Moreover, the simplified method neglects the corresponding torsion by applying uniform distribution wind loads to evaluate maximum shear which may be not sufficient for buildings considered sensitive to torsion. Similarly, Figures 10 and 11 present torsional and shear load cases in the longitudinal direction. For buildings with flat roofs, the simplified method compares well with wind tunnel in predicting the maximum torsion and overestimates maximum shear; while, the simplified method underestimates maximum torsion and successes in predicting maximum shear on buildings with 45° roof angle.

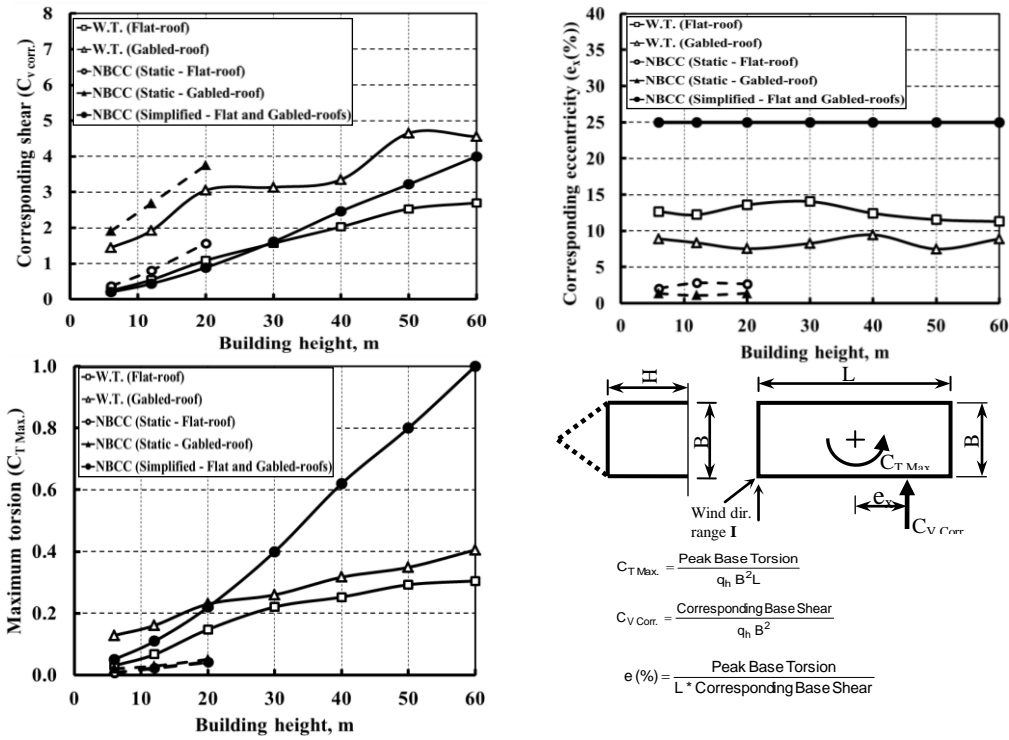


Figure (8). Comparison of torsional load case evaluated by NBCC (2010) and wind tunnel measurements for buildings with 0° and 45° roof angles (Transverse direction)

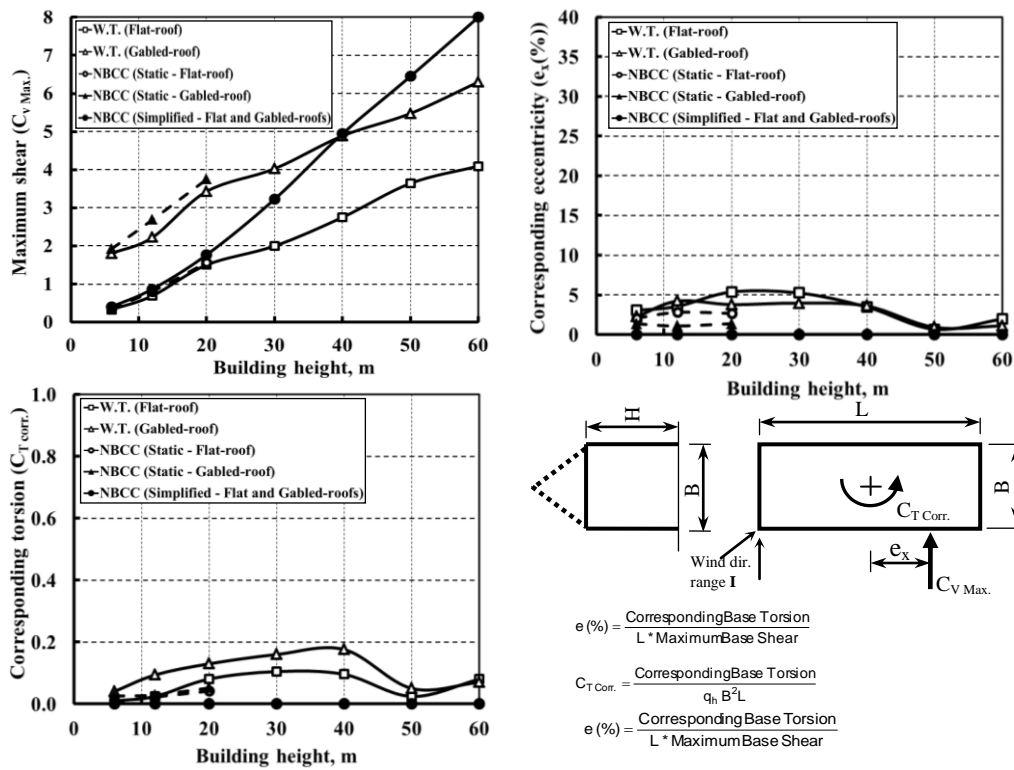


Figure (9). Comparison of shear load case evaluated by NBCC (2010) and wind tunnel measurements for buildings with 0° and 45° roof angles (Transverse direction)

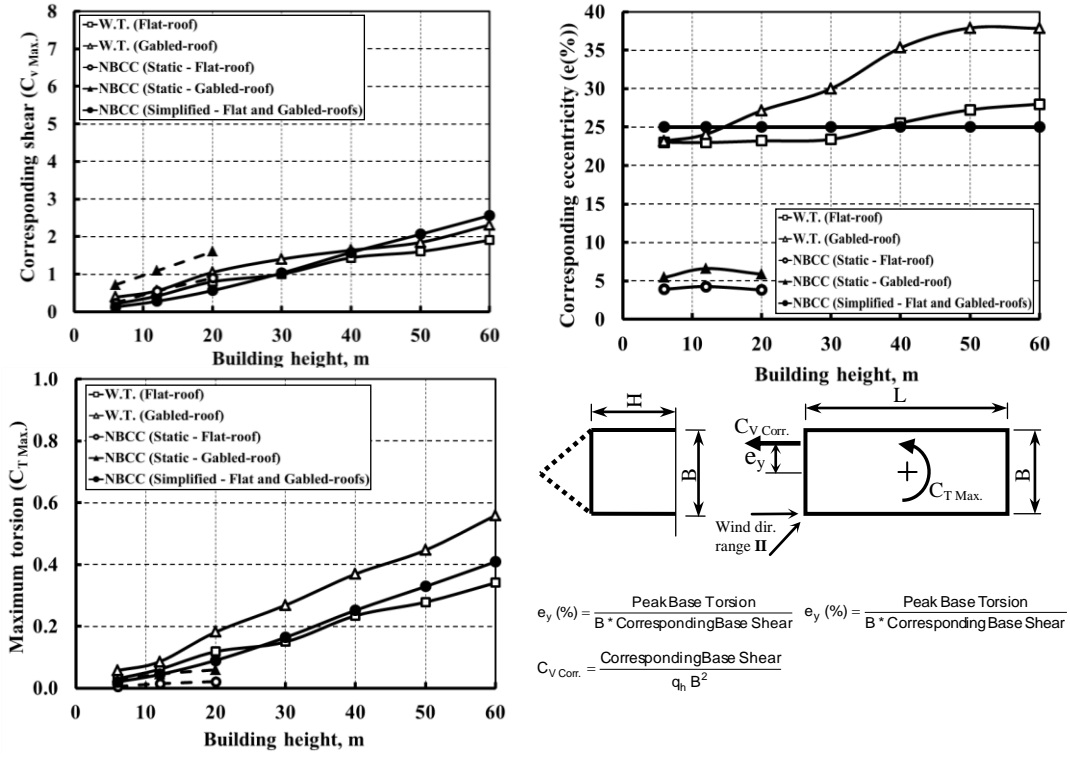


Figure (10). Comparison of torsional load case evaluated by NBCC (2010) and wind tunnel measurements for buildings with 0° and 45° roof angles (Longitudinal direction)

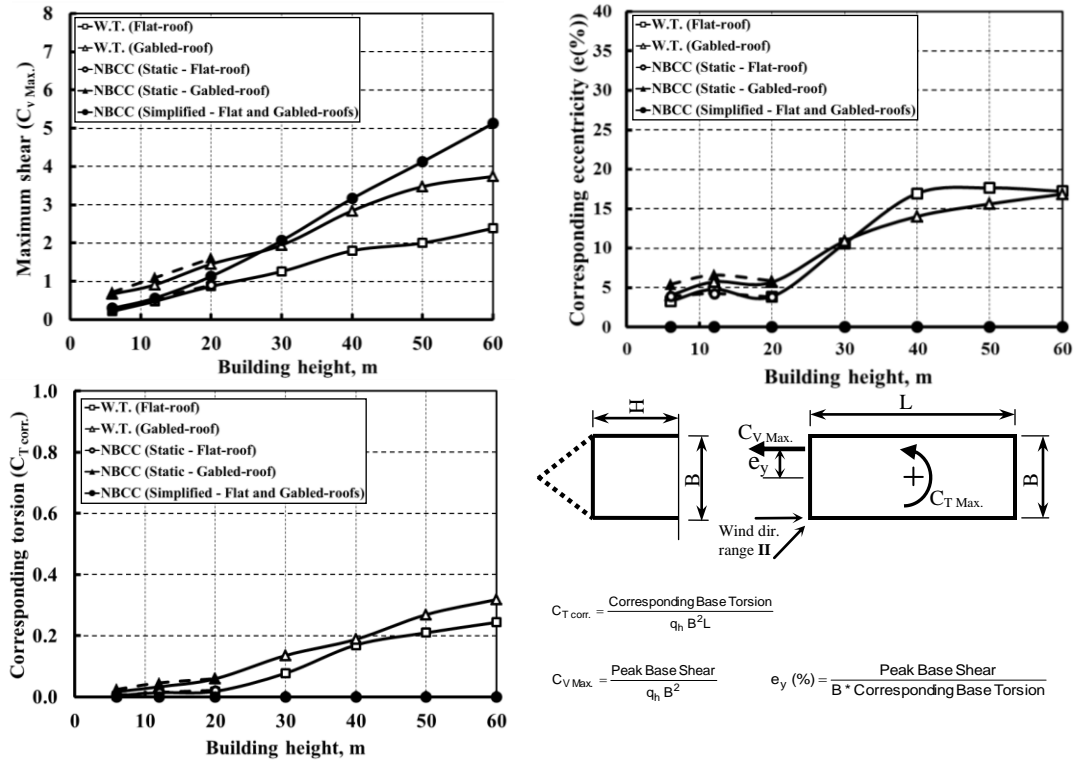


Figure (11). Comparison of shear load case evaluated by NBCC (2010) and wind tunnel measurements for buildings with 0° and 45° roof angles (Longitudinal direction)

8 Conclusion

Wind-induced torsion and shears were measured in the wind tunnel for buildings having the same horizontal dimensions, different roof angles (0° , and 45°) and heights ranging from 6 m to 60 m. In addition, the experimental results were compared with wind load provisions NBCC (2010). The analysis of experimental results and comparisons with codes/standards demonstrate the following:

For low-rise buildings, the static method in the NBCC (2010):

- underestimates torsion significantly;
- compares well with the maximum shear evaluated in the wind tunnel; and
- succeeds to predict corresponding torsion for buildings with flat roofs but not always for buildings with 45° roof angle

For medium-rise buildings, the simplified method in the NBCC (2010):

a- In the Transverse direction:

- overestimates maximum torsion and shear on buildings with flat roofs.
- overestimates maximum torsion and underestimates maximum shear on buildings with roof angle 45° with height up to 40 m.

b- In the Longitudinal direction:

- compares well with wind tunnel in evaluating maximum torsion, while it overestimates maximum shear on buildings with flat roofs.
- underestimates maximum torsion and succeeds to evaluate maximum shear on buildings with roof angle of 45° .

9 ACKNOWLEDGMENT

The authors are grateful for the financial support received for this study from the Natural Sciences and Engineering Research Council of Canada (NSERC), as well as *le Fonds de Recherche du Québec - Nature et Technologies* (FRQNT) and *Centre d'Études Interuniversitaire sur les Structures sous Charges Extrêmes* (CEISCE).

10 References

- Boggs, D. W., Hosoya, N. and Cochran, L. (2000) "Source of torsional wind loading on tall buildings-lessons from the wind tunnel" Proceedings of the Structures Congress, Sponsored by ASCE/SEI, Philadelphia, May
- Elsharawy, M., Stathopoulos, T., and Galal, K. (2012) "Wind-Induced torsional loads on low buildings." *Journal of Wind Engineering and Industrial Aerodynamics*, Vol. 104-106, 40-48
- Isyumov, N., and Case, P. C. (2000) "Wind-Induced torsional loads and responses of buildings." Proceedings of the Structures Congress, Sponsored by ASCE/SEI, Philadelphia, May
- Keast, D.C., Barbagallo, A., and Wood, G.S. (2012) "Correlation of wind load combinations including torsion on medium-rise buildings." *Wind and Structures, An International Journal*, 15(5), 423-439
- Melbourne, W.H. (1975) "Probability distributions of response of BHP house to wind action and model comparisons." *Journal of Wind Engineering and Industrial Aerodynamics*, 1 (2), 167-175
- NBCC (2010) "User's Guide – NBC 2010, Structural Commentaries (part 4)." Issued by the Canadian Commission on Buildings and Fire Codes, National Research Council of Canada
- R. A. Sanni, D. Surry, and A. G. Davenport (1992) "Wind loading on intermediate height buildings." *Canadian journal of civil engineering*, 19,148-163.
- T. Stathopoulos and M. Dumitrescu-Brulotte (1989) "Design recommendations for wind loading on buildings of intermediate height." *Canadian Journal of Civil Engineering*, 16, 910-916.
- Tamura, Y., Kikuchi, H., Hibi, K. (2001) "Extreme wind pressure distributions on low- and middle-rise building models." *Journal of Wind Engineering and Industrial Aerodynamics*, 89 (14-15), 1635-1646
- Tamura, Y., Kikuchi, H., Hibi, K. (2003) "Quasi-static wind load combinations for low- and middle-rise buildings." *Journal of Wind Engineering and Industrial Aerodynamics*, 91, 1613-1625
- Van der Hoven, I. (1957) "Power spectrum of wind velocities fluctuations in the frequency range from 0.0007 to 900 Cycles per hour." *Journal of Meteorology*, 14, 160-164
- Vickery, B.J., Basu, R.I. (1984) "The response of reinforced concrete chimneys to vortex shedding." *Engineering Structures*, 6, 324-333